

Electronic Supplementary Information (ESI)

NIR Light Induced H₂ Evolution by a Metal-free Photocatalyst

Xinyuan Xia, Ning Deng, Guanwei Cui, Junfeng Xie, Xifeng Shi, Yingqiang Zhao,
Qian Wang, Wen Wang and Bo Tang*

College of Chemistry, Chemical Engineering and Materials Science, Collaborative
Innovation Center of Functionalized Probes for Chemical Imaging in Universities of
Shandong, Key Laboratory of Molecular and Nano Probes, Ministry of Education,
Shandong Provincial Key Laboratory of Clean Production of Fine Chemicals,
Shandong Normal University, Jinan, Shandong, 250014 (P.R. China)

E-mail: tangb@sdu.edu.cn

Experimental section

Preparation of bulk g-C₃N₄ and g-C₃N₄ nanosheets (CNNS). Bulk g-C₃N₄ was prepared according to previous literatures.^{1, 2} In detail, melamine (Sigma Aldrich, 99%) was heated to 550 °C for 3 h with a heating rate of 4 °C/min. The resulting yellow agglomerates were milled into powder in a mortar. The g-C₃N₄ nanosheets were synthesized by thermal oxidation etching of the bulk g-C₃N₄.¹ Typically, 400 mg of the bulk g-C₃N₄ placed in an open alumina crucible was heated to 500 °C for 2 h with a heating rate of 5 °C/min. The final product was obtained as a light yellow

powder of g-C₃N₄ nanosheets.

Preparation of carbon quantum dots (CQDs). The CQDs were prepared by the pyrolytic method from EDTA-2Na·2H₂O based on a previous report with some modifications.³ Typically, a quartz boat filled with EDTA-2Na·2H₂O (AR, 0.5 g) was thrust into a quartz tube and calcined at 350 °C for 2 h under N₂ flow. After cooling to room temperature, the resulting black powders were dissolved in ethanol and then centrifuged at a high speed (14000 rpm) for 20 minutes. Pure CQDs powder was obtained by evaporating the upper yellow solution and drying the concentrated solution under vacuum at 70 °C overnight.

Preparation of CNNS/CQDs. The CNNS/CQDs hybrids were constructed by a hydrothermal method. In a typical case, 8 mL distilled water and 8 mL ethanol were mixed together, and then 0.03 g of the as-prepared CNNS and a certain amount of CQDs solution (1mg mL⁻¹, dispersed in ethanol) were added. The mixture was stirring for 30 minutes to form a homogeneous suspension. After that, the suspension was transferred into a 20 mL Teflon-lined autoclave and heated at 180 °C for 4 h. The resulting CNNS/CQDs hybrids were collected by centrifugation and then washed with distilled water three times, and finally dried under vacuum at 50 °C overnight. The CNNS/CQDs hybrids with different contents of CQDs (0, 0.5, 1.0, 5.0, 10 and 15 wt%) were prepared and marked as e. g. CNNS/CQDs-10wt%.

Characterizations. Transmission Electron Microscopy (TEM) and High-Resolution Transmission Electron Microscopy (HRTEM) analyses were carried out on a JEM 2010 EX instrument. The crystal structures of the samples were measured by X-ray diffraction (XRD, Bruker D8, Germany) equipped with Cu K α radiation. The UV/Vis diffuse reflection spectra (DRS) data were taken on a Shimadzu UV-2500 spectrophotometer. Fourier transform infrared (FT-IR) spectra were obtained on a Varian 3100 FT-IR spectrometer. X-ray photoelectron spectroscopy (XPS) measurements were performed on a Thermo Fisher Scientific Escalab 250 X-ray photoelectron spectroscopy using an Al K α ($h = 1486.6$ eV) radiation excitation source. Photoluminescent (PL) spectra were detected by an FLS-920 Edinburgh fluorescence spectrometer. BET measurements were carried out on Micromeritics Tristar 3000. Raman spectrum was collected using an HR 800 Raman spectroscope (J Y, France).

Photoelectrochemical measurements. All the photochemical measurements (Photocurrent, Mott-schottky plots, EIS and CV) were performed by CHI-660D workstation (CH Instruments) in a standard three-electrode system using the prepared samples as the working electrodes with an active area of ca. 2.0 cm^2 , saturated calomel electrode as a reference electrode, and a Pt sheet as the counter electrode. The electrolyte was 0.1 M NaClO_4 aqueous solution (PH = 6.8). Specifically, the working electrodes were prepared by spreading aqueous slurries of samples in terpineol over ITO glass substrate. Next, the electrodes were dried in an oven following by calcining

at 400 °C for 30 min under Argon flow. The thicknesses of all the photocatalyst coatings on the ITO electrodes were almost the same. The light source was a 300 W xenon lamp (UV-Vis) equipped with a cut-off filter (Vis, $\lambda \geq 420$ nm) or an 808 nm laser beam (MDL-III-808) purchased from Changchun New Industries Optoelectronics Tech. Co., Ltd (Changchun, China). The transient photocurrent tests were carried out at a bias of 0.4 V. The cyclic voltammogram (CV) was performed using bare ITO glass as working electrode with a scan rate of 0.1 V s⁻¹ in a CQDs solution (0.11 mg mL⁻¹). The electrochemical impedance spectroscopy (EIS) measurements were performed by applying an AC voltage with 10 mV amplitude in a frequency range from 0.1 Hz to 1MHz under open circuit potential conditions. The perturbation signal for Mott-Schottky measurements was set at 5 mV.

Photocatalytic activity for H₂ evolution. The photocatalytic H₂ production experiments were performed in a 20 mL Pyrex bottle with a rubber septum. 10 mg of the as-prepared photocatalysts were suspended in 10 mL aqueous solution containing 20 vol% methanol as sacrificial electron donor. Prior to photocatalysis experiment, the sample solutions were purged with Ar for 10 minutes to remove the O₂. Each sample was irradiated by a 1000 W xenon lamp (UV-Vis) equipped with a cut-off filter (Vis, $\lambda \geq 420$ nm) or an 808 nm laser beam (MDL-III-808) at room temperature under constant stirring. The amount of evolved H₂ was analyzed by gas chromatography (FULI 9750, TCD, Ar as the carrier gas, and 5 Å molecular sieve column).

External quantum efficiency (EQE) spectra. The EQE measurements were performed in a 200 mL Pyrex bottle with a rubber septum. 200 mg of the as-prepared photocatalysts were suspended in 150 mL aqueous solution containing 20 vol% methanol as sacrificial electron donor. Prior to photocatalysis experiment, the sample solutions were purged with Ar for 10 minutes to remove the O₂. Each sample was irradiated by a 300 W xenon lamp equipped with a set of $\lambda_0 \pm 15$ nm band-pass filters (λ_0 =405, 435, 500, 550, 600, 650 and 700 nm) and an 808 nm laser beam (MDL-III-808) of which all the irradiation intensities were determined by a NOVA II laser power meter (Ophir Photonics). The number of incident photons (N) is calculated by equation (1) and the EQE is calculated from equation (2).

$$N = \frac{E\lambda}{hc} \quad (1)$$

$$EQE = \frac{2 * \text{the number of evolved H}_2 \text{ molecules}}{\text{the number of incident photons}} \quad (2)$$

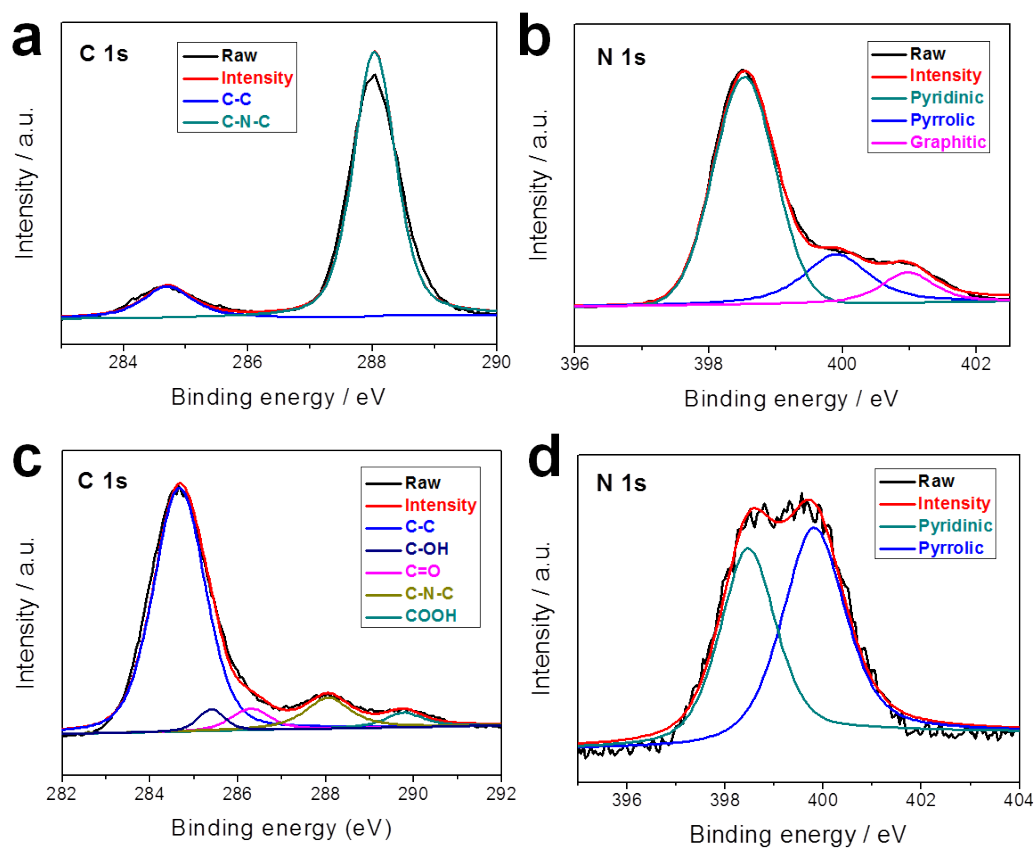


Fig. S1 High resolution XPS spectra of C 1s (a, c) and N 1s (b, d) for a, b) bare CNNS c, d) as-prepared CQDs.

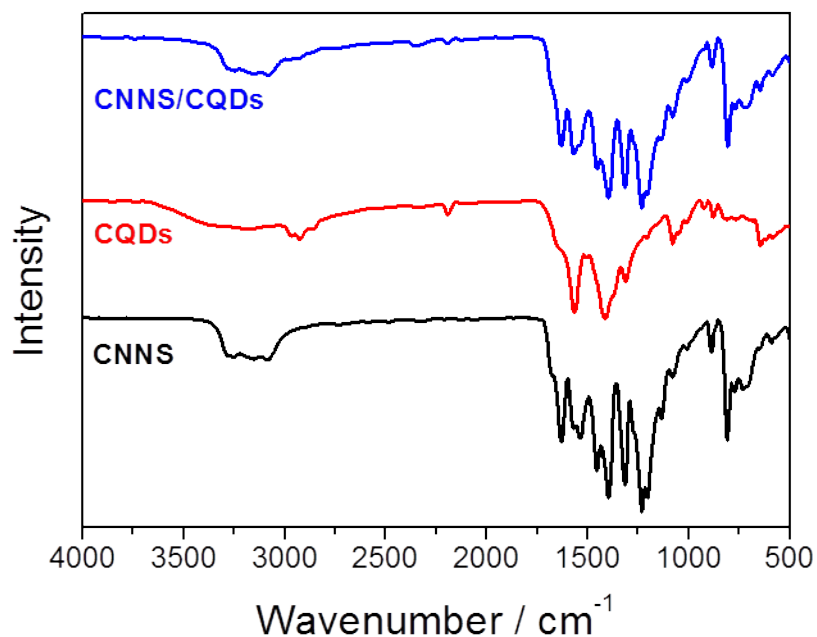


Fig. S2 FTIR spectra of CNNS, CQDs and CNNS/CQDs.

FTIR spectra were recorded and presented in Fig. S3. For bare CNNS, the characteristic sharp peak of polymeric melon emerges at around 810 cm^{-1} and in the regions of 900 to 1800 cm^{-1} and 3000 to 3600 cm^{-1} .^{1, 4} CQDs are denoted to be rendered with carbonyl, carboxyl and hydroxyl groups on their surfaces from the predominant peaks for C=O (1566 cm^{-1}), C-OH (1312 cm^{-1}) and -OH (3199 cm^{-1}).⁵ The FTIR spectrum of CNNS/CQDs is generally identical with that of bare CNNS probably due to the similar peak positions for CNNS and CQDs and low CQDs deposition content, ensuring that no other impurities are introduced into the CNNS/CQDs products during the hydrothermal deposition process.

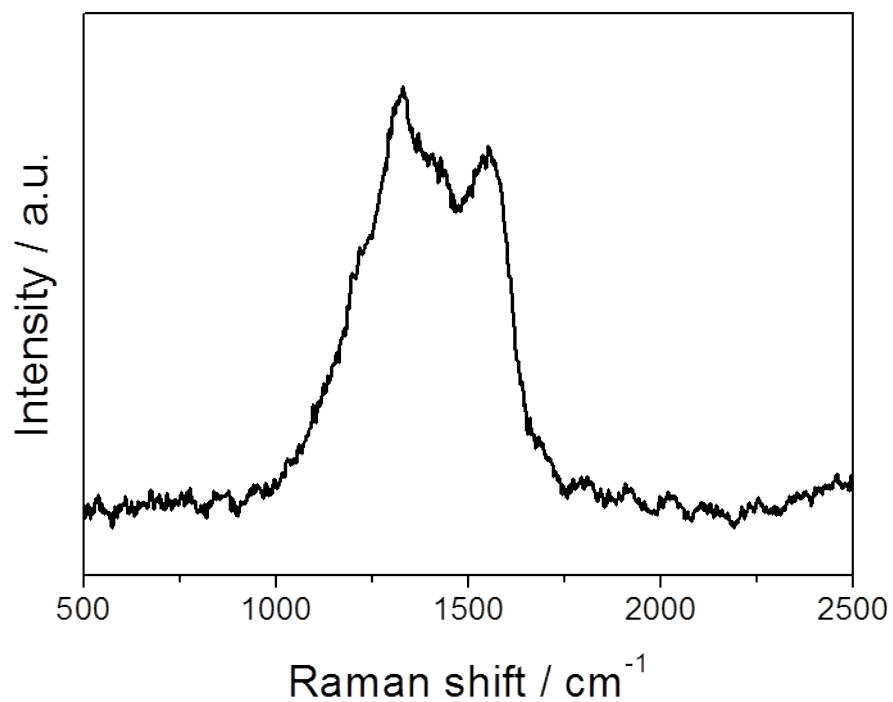


Fig. S3 Raman spectrum of CQDs.

The Raman spectrum of CQDs (Fig. S3) shows typical graphitic D band at 1330 cm⁻¹ and G band at 1552 cm⁻¹, ascribed to disordered sp³ carbon and conjugated sp² clusters, respectively.

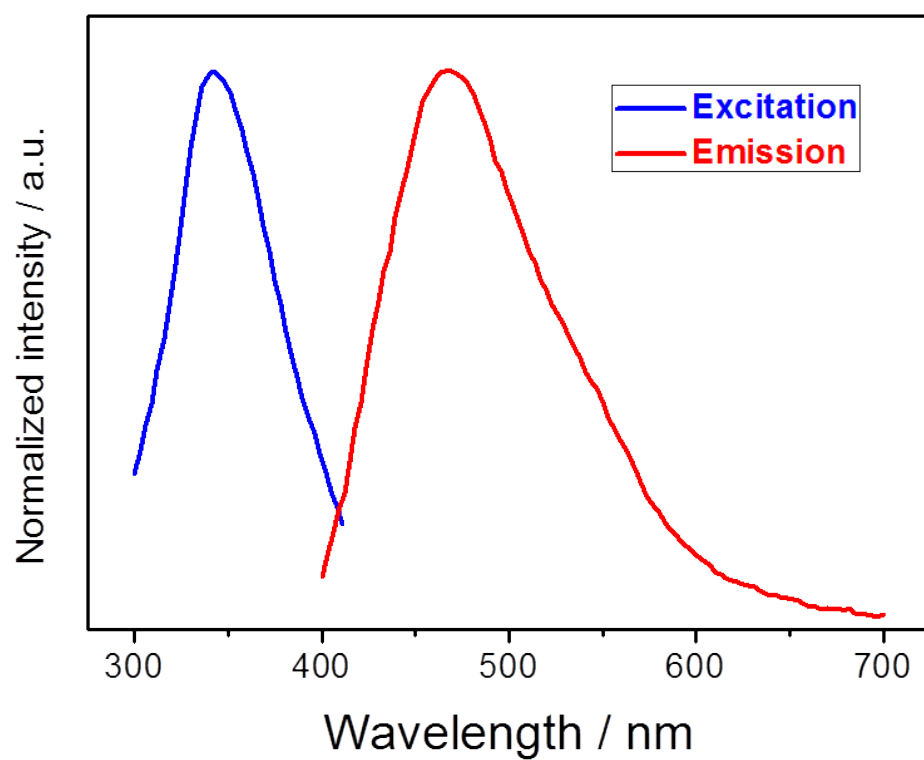


Fig. S4 Normalized PL spectra of CQDs (excitation and emission) measured in an ethanol solution of CQDs (2.5 mg mL^{-1}).

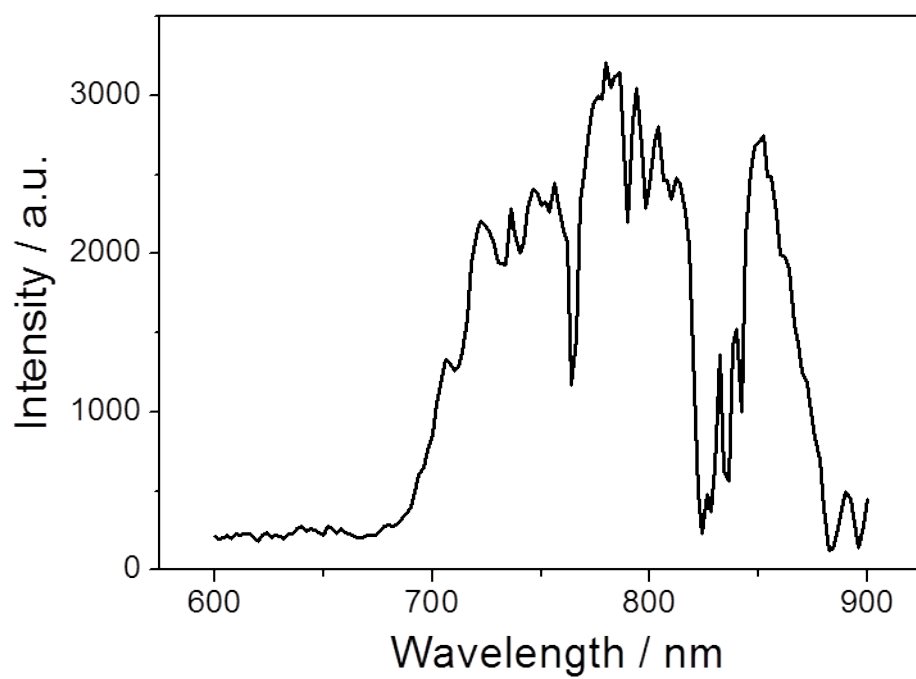


Fig. S5 Upconversion PL excitation spectrum of CQDs associated with the strongest luminescence at 470 nm measured in an ethanol solution of CQDs (2.5 mg mL^{-1}).

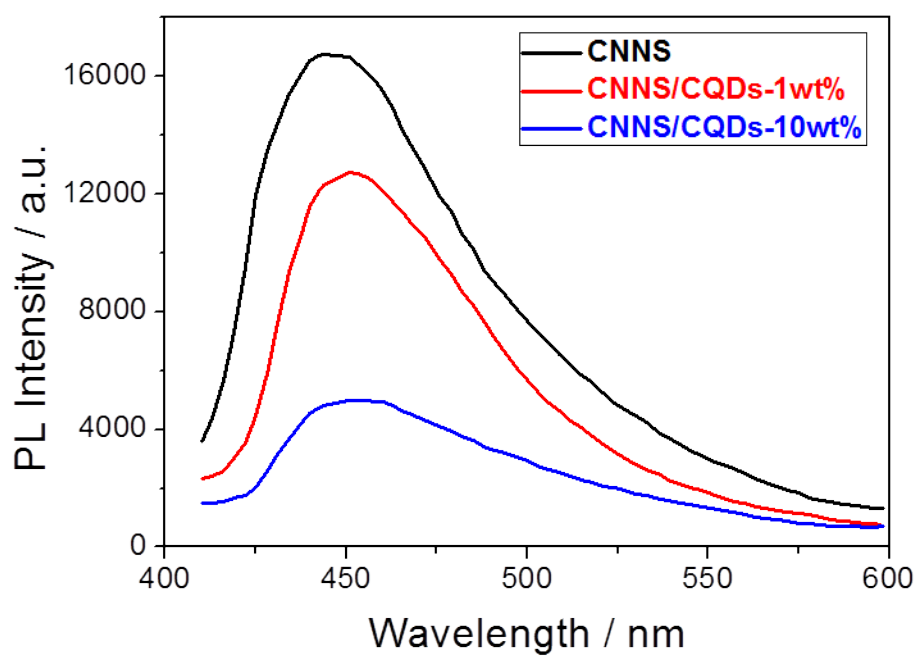


Fig. S6 PL spectra of CNNS, CNNS/CQDs-1wt% and CNNS/CQDs-10wt% under 310 nm excitation.

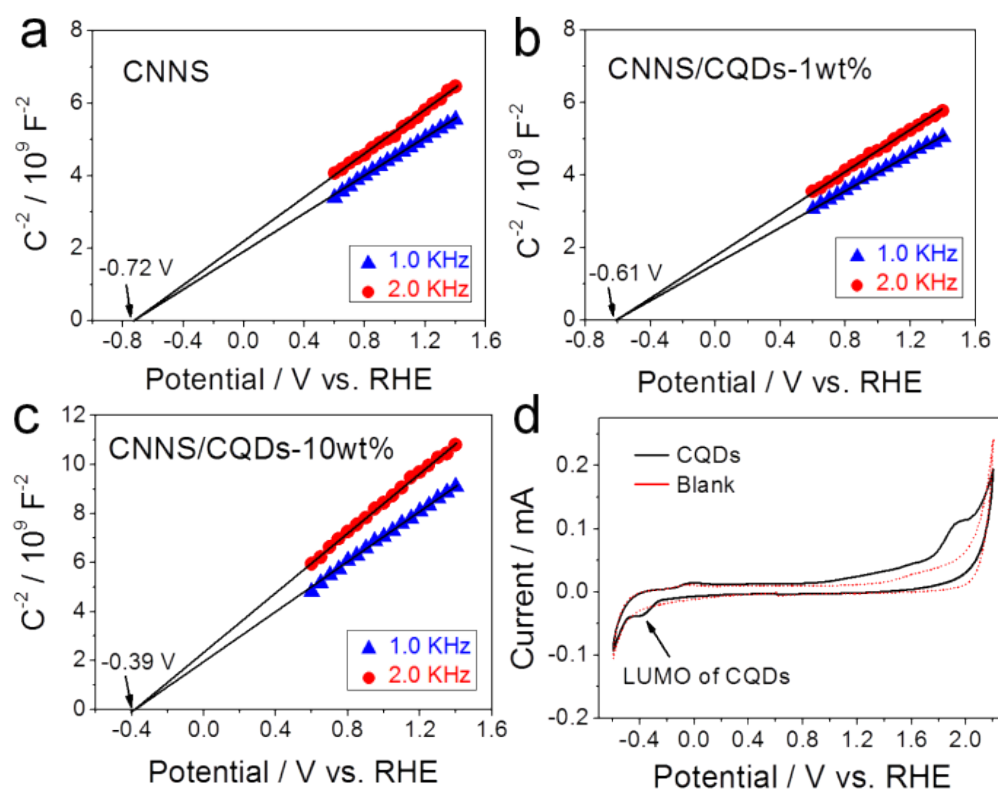


Fig. S7 (a-c) Mott-Schottky plots. (d) CV curves of CQDs.

Table S1 External quantum efficiency (EQE) at difference wavelengths of catalysts with low- and high-content CQDs loading.

EQE(%) λ (nm)	CNNS/CQDs-1wt%	CNNS/CQDs-10wt%
405	1.400	0.608
435	0.498	0.236
500	0.192	0.164
550	0.110	0.090
600	0.064	0.066
650	0.054	0.048
700	0	0.024
808	0	0.034

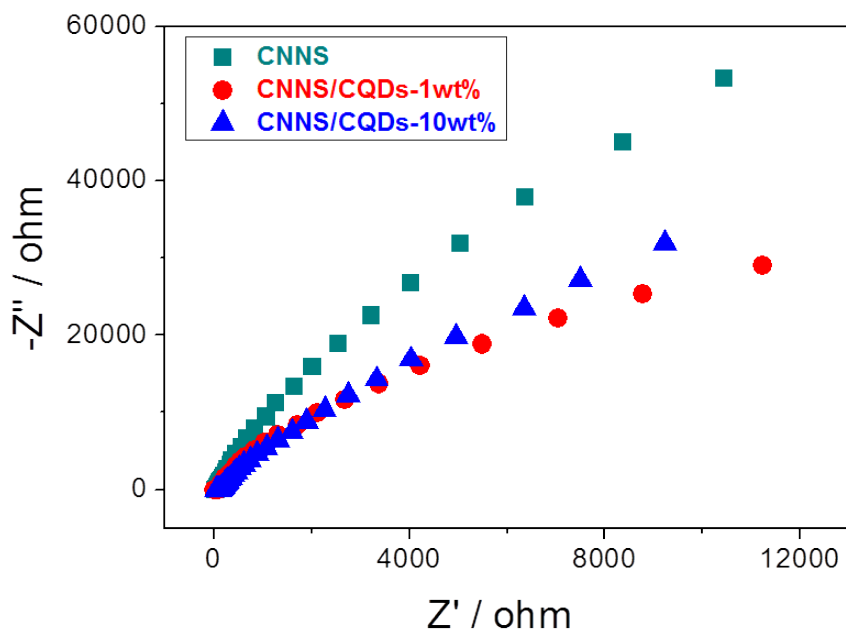


Fig. S8 Electrochemical impedance spectroscopy (EIS) Nyquist plots of CNNS, CNNS/CQDs-1wt% and CNNS/CQDs-10wt% under UV-Vis light irradiation.

Further information on the photocatalytic mechanism is provided by electrochemical impedance spectroscopy (EIS) recorded under UV-Vis light (Fig. S7). The charge-transfer rates of photocatalysts display typical semicircular Nyquist plots for each catalyst, in which remarkably decreased arc radii are obtained for both CNNS/CQDs-1wt% and CNNS/CQDs-10wt% compared to that of bare CNNS. The result demonstrates that CQDs deposition leads to increased photoinduced charges and promoted interfacial charge separation and migration that efficiently reduce exciton quenching and energy dissipation. In addition, CNNS/CQDs-1wt% is revealed to have a bit smaller arc radius than CNNS/CQDs-10wt%, probably due to that the accumulation of CQDs led by high deposition content may to some extent hinder the charge transfer to get a higher impedance.

References

- 1 P. Niu, L. Zhang, G. Liu and H.-M. Cheng, *Adv. Funct. Mater.*, 2012, **22**, 4763-4770.
- 2 X. Wang, K. Maeda, A. Thomas, K. Takanabe, G. Xin, J. M. Carlsson, K. Domen and M. Antonietti, *Nat. Mater.* , 2009, **8**, 76-80.
- 3 D. Pan, J. Zhang, Z. Li, C. Wu, X. Yan and M. Wu, *Chem. Commun.* , 2010, **46**, 3681-3683.
- 4 S. Yang, Y. Gong, J. Zhang, L. Zhan, L. Ma, Z. Fang, R. Vajtai, X. Wang and P. M. Ajayan, *Adv. Mater.* , 2013, **25**, 2452-2456.
- 5 H. Yu, Y. Zhao, C. Zhou, L. Shang, Y. Peng, Y. Cao, L.-Z. Wu, C.-H. Tung and T. Zhang, *J. Mater. Chem. A*, 2014, **2**, 3344.